HHS Public Access

Author manuscript

Cell. Author manuscript; available in PMC 2016 September 10.

Published in final edited form as:

Cell. 2015 September 10; 162(6): 1217–1228. doi:10.1016/j.cell.2015.08.012.

Phosphoenolpyruvate Is a Metabolic Checkpoint of Anti-tumor T Cell Responses

Ping-Chih Ho[1,*], **Jessica Dauz Bihuniak**[2], **Andrew N. Macintyre**[3], **Matthew Staron**[1], **Xiaojing Liu**[4], **Robert Amezquita**[1,5], **Yao-Chen Tsui**[1,6], **Guoliang Cui**[1], **Goran Micevic**[7], **Jose C. Perales**[8], **Steven H. Kleinstein**[5], **E. Dale Abel**[9], **Karl L. Insogna**[2], **Stefan Feske**[10], **Jason W. Locasale**[4], **Marcus W. Bosenberg**[5,7], **Jeffrey C. Rathmell**[3], and **Susan M. Kaech**[1,6,*]

[1]Department of Immunobiology, Yale University School of Medicine, New Haven, CT 06519, USA

[2]Department of Internal Medicine, Yale University School of Medicine, New Haven, CT 06519, USA

[3]Department of Pharmacology and Cancer Biology, Immunology, Duke Molecular Physiology Institute, Duke University, Durham, NC 27710, USA

[4]Division of Nutritional Sciences, Cornell University, Ithaca, NY 14853, USA

[5]Department of Pathology, Yale University School of Medicine, New Haven, CT 06519, USA

[6]Howard Hughes Medical Institute, Chevy Chase, MD 20815, USA

[7]Department of Dermatology, Yale University School of Medicine, New Haven, CT 06519, USA

[8]Biophysics Unit, Department of Physiological Sciences II, IDIBELL-University of Barcelona, Fexia Llarga s/n 08907, Spain

[9]Fraternal Order of Eagles Diabetes Research Center, Division of Endocrinology and Metabolism, Department of Medicine, Carver College of Medicine University of Iowa, Iowa City, IA 52242, USA

[10]Department of Pathology, New York University Langone Medical Center, New York, NY 10016, USA

SUMMARY

Activated T cells engage aerobic glycolysis and anabolic metabolism for growth, proliferation, and effector functions. We propose that a glucose-poor tumor microenvironment limits aerobic glycolysis in tumor-infiltrating T cells, which suppresses tumoricidal effector functions. We

[*]Correspondence: ping-chih.ho@unil.ch (P.-C.H.), susan.kaech@yale.edu (S.M.K.).

AUTHOR CONTRIBUTIONS

P-C.H., S.M.K., J.D.B., K.L.I., and A.N.M. designed the research. P-C.H., J.D.B., A.N.M., X.L., M.S., Y-C.T., G.C., R.A. G.M., M.W.B. and S.H.K. performed the experiments and bioinformatics analyses. J.C.P. and E.D.A. provided critical reagents. P-C.H., J.W.L., J.C.R., S. F., and S.M.K. analyzed the results. P-C.H. and S.M.K. wrote the manuscript.

ACCESSION NUMBERS

The accession number for the RNA-seq data reported in this paper is SRA: SRP058700.

SUPPLEMENTAL INFORMATION

Supplemental Information includes Supplemental Experimental Procedures and six figures and can be found with this article online at http://dx.doi.org/10.1016/j.cell.2015.08.012.

discovered a new role for the glycolytic metabolite phosphoenolpyruvate (PEP) in sustaining T cell receptor-mediated Ca^{2+}-NFAT signaling and effector functions by repressing sarco/ER Ca^{2+}-ATPase (SERCA) activity. Tumor-specific CD4 and CD8 T cells could be metabolically reprogrammed by increasing PEP production through overexpression of phosphoenolpyruvate carboxykinase 1 (PCK1), which bolstered effector functions. Moreover, PCK1-overexpressing T cells restricted tumor growth and prolonged the survival of melanoma-bearing mice. This study uncovers new metabolic checkpoints for T cell activity and demonstrates that metabolic reprogramming of tumor-reactive T cells can enhance anti-tumor T cell responses, illuminating new forms of immunotherapy.

Graphical Abstract

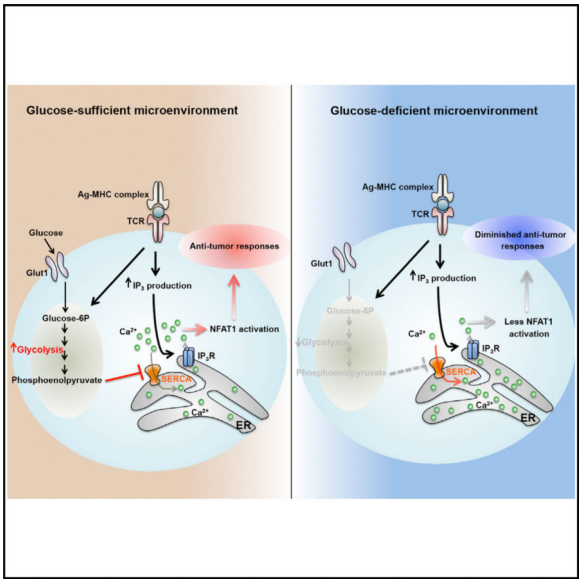

INTRODUCTION

Host immunity provides wide spectrum protection that serves to eradicate cancerous cells in addition to infectious pathogens. Multiple types of immune cells are involved in tumor immunosurveillance and of particular importance are the tumor-infiltrating lymphocytes (TILs) (i.e., T cells) (Braumüller et al., 2013; Shiao et al., 2011). In most established tumors, however, the tumoricidal effector functions of TILs such as IFNγ production and cytotoxicity are restricted by multiple environmental factors. This includes the accumulation of immunoregulatory cells such as regulatory CD4+ T cells (Tregs), myeloid derived suppressor cells (MDSCs) and tolerogenic antigen-presenting cells (APCs) (Mellman et al., 2011; Shiao et al., 2011). Additionally, alterations in the availability of nutrients (e.g., lactate and tryptophan-related metabolites such as kynurenine) in the tumor microenvironment can limit TIL activity (Yang et al., 2013). Another prominent feature of TILs is the increased expression of inhibitory checkpoint receptors (e.g., programmed cell death protein 1 [PD-1], lymphocyte-activation gene 3 [Lag3], and cytotoxic T-lymphocyte-associated protein 4 [CTLA-4]) that desensitizes T cell receptor (TCR) signaling and contributes to their functional impairment (Baitsch et al., 2012). T cells displaying such

properties are commonly referred to as “functionally exhausted” (Wherry, 2011). These discoveries have led to the development of cancer immunotherapies that reawaken exhausted TILs by blocking inhibitory checkpoint receptors such as PD-1 or CTLA-4 or targeting other immunoregulatory cells. Adoptive cell therapy (ACT) of tumor-specific T cells is another promising form of anti-cancer immunotherapy that increases the repertoire of cytotoxic T cells to eradicate established tumors. ACT has the added benefit of permitting genetic modifications of TILs to express proteins that could aide in tumor destruction (Maude et al., 2014). These breakthroughs demonstrate that tumor immunotherapy holds great promise (Callahan et al., 2010; Wolchok et al., 2013), but also present us with challenges to devise additional treatment options in conjunction with those currently available to further increase patient objective responses. To meet these challenges, we must gain a clearer understanding of what causes T cell exhaustion in tumors, and we hypothesize that the metabolic states of the TILs and tumor cells, as well as other cell types in the tumor microenvironment, are principal components of this process.

Deregulated anabolic metabolism and increased rates of aerobic glycolysis (i.e., the Warburg effect), glutaminolysis and fatty acid synthesis are cardinal features of most tumor cells that fuels their growth and proliferation (Hanahan and Weinberg, 2011; Ward and Thompson, 2012). Interestingly, activated T lymphocytes undergo a metabolic switch similar to cancer cells and upregulate aerobic glycolysis and glutaminolysis to permit proliferation and differentiation into specialized effector T cells. Given their similarities in metabolic profiles and nutrient requirements, it is possible that the abnormally high metabolic rates and consumption of nutrients by tumor cells competes with neighboring T cells, which leads to T cell metabolic exhaustion that underlies their functional exhaustion. Supporting this notion, reports have shown that the concentration of extracellular glucose are lower in tumors compared to healthy tissues (Gullino et al., 1964). Thus, limited glucose availability could be an environmental restriction that promotes T cell exhaustion, and if true, it is important to learn how this affects T cell receptor (TCR) signaling and effector functions in tumors. Perhaps, new therapies directed at reprogramming T cell metabolism could be developed to enhance their functional fitness in the tumor microenvironment.

TCR stimulation activates numerous key signaling pathways that coordinately induce anabolic metabolism, aerobic glycolysis, and effector T cell proliferation and differentiation (Smith-Garvin et al., 2009). Increased aerobic glycolysis is essential for the production of biosynthetic precursors that fuel effector T cell proliferation and production of effector molecules like IFNγ, IL-2, and IL-17 and Granzyme B in T cells (Cham et al., 2008; Chang et al., 2013; Finlay et al., 2012; Michalek et al., 2011). Activation of PI3K, Akt, and mTOR triggers the switch to anabolic metabolism by inducing transcription factors such as Myc and hypoxia-inducible factor 1 (HIF1) (MacIver et al., 2013; Wang et al., 2011a). T cells rendered functionally anergic that are unable to activate Ca^{2+} and nuclear factor of activated T cells (NFAT) signaling show diminished rates of aerobic glycolysis and anabolic metabolism following stimulation (Srinivasan and Frauwirth, 2007; Zheng et al., 2009). Similarly, CD8 T cells with increased PD-1 expression fail to fully activate mTOR or aerobic glycolysis following TCR stimulation and conversely, those with hyper-HIF1α activity and aerobic glycolysis are refractory to functional exhaustion (Doedens et al., 2013; Parry et al., 2005; Staron et al., 2014). The glycolytic enzymes may also serve direct roles in

regulating effector functions in T cells because recent work showed that when glycolytic rates are low, the glyceralde-hyde phosphate dehydrogenase (GAPDH) binds to and suppresses Ifng mRNA translation in T cells (Chang et al., 2013; Gubser et al., 2013). These findings demonstrate strong interconnections between T cell metabolism and effector functions but little remains known about how metabolic pathways or their metabolites fine-tune T cell activity.

In this study, we found that intratumoral CD4 T cells displayed signs of glucose deprivation and diminished anti-tumor effector functions, suggesting that a glucose-poor tumor microenvironment might contribute to TIL exhaustion. Furthermore, increased expression of hexokinase 2 (HK2) in tumor cells allowed for more efficient evasion of CD4 T cell-mediated immune surveillance indicating that a metabolic competition could exist between TILs and tumor cells. Linking glucose-deprivation to T cell function, we also discovered that insufficiency of the glycolytic metabolite phosphoenolpyruvate (PEP) led to defects in Ca^{2+}-NFAT signaling and T cell activation by increasing SERCA-mediated Ca^{2+} re-uptake. Most importantly, we provided proof-of-concept evidence that metabolic reprogramming of T cells to increase PEP production could be a promising strategy to elevate T cell mediated anti-tumor immune responses and improve the effects of adoptive T cell transfer immunotherapy.

RESULTS

Glucose limitation suppresses anti-tumor effector functions of intratumoral TH1 CD4 T cells while stimulating TGFβ production.

To investigate whether limited glucose availability within the tumor microenvironment suppressed aerobic glycolysis and hence, effector functions in TILs, we first compared the concentration of glucose in the interstitial fluid of the spleen, blood, and tumors from melanoma-bearing Tyr-creERT2/BrafV600E/Ptenlox (Braf/Pten) mice (Dankort et al., 2009) (Figure 1A) and B16 melanoma-bearing mice (data not shown). As reported in other solid tumors (Gullino et al., 1964), the glucose level of the tumor interstitial fluid (~0.6 mM) was approximately ten times lower than that of the spleen and blood (~9 mM). Additionally, intratumoral CD44hi CD25lo CD4+ T cells (i.e., activated non-Treg CD4+ T cells) failed to take-up glucose as efficiently as their counterparts in the spleen based on intracellular staining with the fluorescent glucose analog 2-NBDG (Figure 1B). We further assessed 2NDBG-uptake in tumor infiltrating non-Treg CD4+ T cells, Tregs, tumor-associated macrophages (TAMs), and MDSCs. This showed that non-Treg CD4+ T cells take-up marginally less 2NDBG than TAMs, but not MDCSs. Unexpectedly, the intramoral and splenic Tregs demonstrated higher 2NDBG uptake compared to the other cell populations (Figure S1A). Furthermore, co-culturing TH1 CD4+ T cells with Braf/Pten melanoma cells demonstrated that the presence of tumor cells could reduce glucose uptake by TH1 cells (Figure 1C), suggesting that tumor cells may directly restrict glucose availability for TILs. As there is no facile way to directly and specifically measure rates of glycolysis in TILs in vivo or in situ, we attempted to determine if intratumoral CD4+ T cells express genes induced by glucose deprivation. We identified a “glucose-deprivation transcriptional signature” in CD4+ T cells by comparing the differentially expressed genes of activated

TH1 cells cultured in high (10 mM) or low (0.1 mM) glucose concentrations using RNA-sequencing and microarrays (Figure S1B), and observed that intratumoral CD4+ T cells expressed higher levels of the glucose-deprived signature genes than CD4+ T cells in the draining lymph nodes (dLNs) (Figure 1D). This result suggested that some portion of the CD4+ TILs experienced glucose-deprivation within the tumor microenvironment in vivo.

Next, we stimulated functional TH1 CD4+ T cells (isolated from lymphocytic choriomeningitis virus (LCMV)-infected animals) in different concentrations of glucose (ranging from 0.1–10 mM) to directly interrogate the effects of glucose deprivation on production of CD40 ligand (CD40L) and IFNγ—two factors critical for maintaining an immunostimulatory microenvironment in the Braf/Pten melanomas (Ho et al., 2014). This showed that these effector functions were suppressed by limited amounts of glucose (Figure 1E). Conversely, glucose deprivation augmented TGFβ production in activated CD4+ T cells (Figure 1F), suggesting that glucose deprivation can cause CD4+ T cells to switch from immuno-supportive to immuno-suppressive states. Importantly, the CD4+ T cells isolated directly ex vivo from melanomas displayed similar functional attributes to the in vitro glucose-deprived TH1 cells. For example, the percentage of CD44hi CD25lo (non-Treg) CD4+ T cells that produced IFNγ or CD40L in the tumors was ~50% lower than that in the spleen or dLN (Figure 1G). Additionally, the expression of the TGFβ latency associated peptide (LAP), a surrogate marker for cells competent to produce TGFβ, was examined on the CD4+ T cells (Figures 1H–IJ), and this showed that a greater proportion of non-Treg CD4+ T cells expressed elevated LAP compared to the FoxP3+ Tregs in both the tumors and dLNs (Figure 1J). Collectively, these data demonstrate that CD4+ TILs display genetic and functional features associated with glucose-deprivation and suggest that competition between tumor cells and TILs for glucose in the tumor microenvironment could contribute to an immunosuppressive environment.

Increased Rates of Aerobic Glycolysis in Melanoma Cells Suppress CD4+ T Cell-Mediated Immunosurveillance

Increased rates of aerobic glycolysis and expression of glycolytic enzymes (e.g., hexokinase 2 [Hk2]) are common hallmarks of cancer cells (Hanahan and Weinberg, 2011), and this may lead to glucose-deprivation and T cell dysfunction in tumors as suggested by the data above. To investigate this hypothesis further, we analyzed the expression of effector T cell genes (e.g., Ifnγ and αvδ Cd40lg) and markers of glycolysis (e.g., Hk2) mRNA within the tumors of 384 melanoma patients (data obtained from The Cancer Genome Atlas [TCGA]) (Cerami et al., 2012; Gao et al., 2013). Interestingly, this showed that the amount of Cd40lg and Ifng mRNA inversely correlated with Hk2 mRNA (Figure S2A). To more directly test if the glycolytic rates of tumor cells affect tumor immunosurveillance by CD4+ T cells, we established stable clones of the Braf/Pten melanoma cell line (YUMM1.7) that expressed either a control vector or one overexpressing HK2 (HK2-OE). As expected, HK2-OE tumor cells had higher rates of aerobic glycolysis than the control cells based on extracellular acidification rates (ECAR) using the Seahorse Extracellular Flux Analyzer (Figure S2B) and HK2-OE tumor cells more efficiently suppressed glucose uptake of TH1 CD4+ T cells in the co-culture assay (Figure S2C). Then we engrafted control and HK2-OE melanoma cell lines into the left and right flanks, respectively, of wild-type C57BL/6 mice. Two weeks later, the

production of CD40L and IFNγ by CD4+ TILs restimulated directly ex vivo was assessed and compared to CD4+ T cells isolated from the control melanomas, those isolated from HK2-OE tumors had lower production of CD40L and IFNγ (Figures 2A and 2B and S2D). This Τηισ φινδινγ strongly suggested that T cell effector functions could be affected by the rates of tumor cell aerobic glycolysis. Next, we compared the growth rates of control and HK2-OE melanoma cell lines engrafted into the left and right flanks, respectively, of Rag1-KO mice that were either reconstituted with CD4+ T cells or not. In accord with higher rates of aerobic glycolysis, the HK2-OE melanomas grew faster compared to the control tumors in both groups of mice (Figure 2C). However, the presence of CD4+ T cells potently suppressed the growth of control melanoma cells, but had little effect on the HK2-OE melanoma cells (Figures 2C–2E). Taken together, these results support the intriguing model that tumor cells with increased rates of aerobic glycolysis are better able to evade anti-tumor CD4+ T cell responses.

Glucose Deprivation Suppresses TCR-Dependent Activation of Ca^{2+} and NFAT Signaling

To better understand how glucose deprivation alters TH1 cell functions, we examined how glycolysis affects TCR signaling after TCR stimulation using several approaches. First, we observed that the induction of the immediate early gene Nur77 (as measured using a Nur77-eGFP reporter that reads out TCR signaling in a Ca^{2+}-dependent manner; Moran et al., 2011) was suppressed in glucose-poor conditions or in the presence of 2-DG (Figure 3A). In contrast, the amount of phosphorylated ERK1/2 (pERK1/2) or AKT (pAKTS473 and pAKTT308) was minimally affected following activation of TH1 CD4 T cells in glucose-deprived conditions (Figure S3). The defect in Nur77 induction prompted us to more closely monitor cytoplasmic calcium flux using the ratiometric Ca^{2+}-sensitive dyes (Fluo-4 and Fura-Red) and flow cytometry, and this revealed that glucose deprivation profoundly repressed TCR-induced Ca^{2+} flux in activated TH1 cells (Figure 3B). Moreover, reducing aerobic glycolysis in activated TH1 cells by glucose deprivation or deletion of the glucose transporter 1 (Macintyre et al., 2014) also suppressed ionomycin-induced cytoplasmic Ca^{2+} accumulation (Figures 3C and 3D). This latter result indicated that the defect in Ca^{2+} flux could be IP3-independent because ionomycin triggers Ca^{2+} efflux from the ER in an IP3-independent manner. In agreement, glucose deprivation did not affect TCR-induced phosphorylation of PLCγ-1 in TH1 cells (Figure 3E). Altogether, these results suggested that glucose-deprivation dampened the magnitude of TCR-induced Ca^{2+} flux, and consequently CD4+ T cell effector functions.

Interestingly, anergic T cells, which have similar functional defects to those observed with glucose-deprivation, also display defects in Ca^{2+} signaling (Schwartz, 2003). Other work has shown that the reduced Ca^{2+} signaling in anergic CD8 T cells impairs the nuclear localization of NFAT1, but not that of NFAT2, indicating differential sensitivity to cytoplasmic Ca^{2+} levels between these two transcription factors (Srinivasan and Frauwirth, 2007). These phenotypes prompted us to examine the cellular distribution of NFAT1 and 2 and expression of anergy-associated genes in glucose-deprived TH1 cells (Safford et al., 2005). In agreement with the prior study (Srinivasan and Frauwirth, 2007), nuclear translocation of NFAT1, but not NFAT2, was severely compromised in glucose-deprived TH1 cells (Figure 3F). Importantly, 5 hr of glucose deprivation led to increased expression

of several “anergy” signature genes, including Egr2, Egr3, IRF4, Hspa1a, Gadd45b, and NFATc1 as previously described (Figure 3G, note the augmented expression of some of these genes in TILs in Figure 1D) (Safford et al., 2005). Collectively, these results identified that glycolysis is critical for sustaining high amounts of Ca^{2+}-NFAT signaling in TH1 cells and that glucose-deprivation results in CD4 T cell dysfunction and expression of anergy-associated genes.

Glycolysis Modulates SERCA-Mediated ER Calcium Uptake Activity

Stimulation of the TCR initially triggers Ca^{2+} efflux from the ER, which subsequently induces extracellular Ca^{2+} import via the calcium-release-activated calcium (CRAC) channel (Feske et al., 2012). To distinguish ER Ca^{2+} efflux from extracellular Ca^{2+} influx, we stimulated CD4+ T cells in the presence or absence of 2-DG with ionomycin in Ca^{2+}-free or Ca^{2+}-containing media and found that 2-DG treatment diminished ionomycin-induced cytosolic accumulation in either condition (Figure 4A, compare red and blue lines in left and right). This suggested that glycolysis is important for maintenance of cytosolic Ca^{2+} levels to support T cell activation. Several Ca^{2+} channels expressed on the plasma membrane (plasma membrane Ca^{2+} ATPase: PMCA), mitochondrial membrane (mitochondrial Ca^{2+} uniporter: MCU), and ER membrane (SERCA) could lower cytosolic Ca^{2+} levels, so we next tested if blocking these Ca^{2+} channels could restore Ca^{2+} flux in glucose-deprived T cells. In contrast to blocking PMCA and MCU channels, treatment with the SERCA inhibitor thapsigargin (Tg) increased Ca^{2+} flux in 2-DG treated or Glut1-KO CD4+ T cells (compare blue and green lines, Figures 4A and 4B and Figure S4). This result suggested that glucose-deprived T cells have increased SERCA activity that suppressed maximal Ca^{2+} flux. Importantly, Tg treatment also restored nuclear translocation of NFAT1 (Figure 4C) as well as IFNγ and CD40L production (Figure 4D) in 2-DG treated TH1 cells. Western blotting of Jurkat T cells showed that 2-DG treatment did not affect the overall amounts of SERCA compared to control cells (Figure 4E), suggesting that the increase in ER Ca^{2+} re-uptake stemmed from increased SERCA activity. Indeed, measurement of radio-labeled Ca^{2+} uptake in ER vesicles isolated from Jurkat T cells revealed that 2-DG treatment increased SERCA-dependent Ca^{2+} uptake by ~2-fold compared to the control cells (Figure 4F). Taken together, these findings strongly indicate that glycolysis suppresses SERCA activity and consequently, glucose deprivation leads to defective Ca^{2+}-NFAT signaling and effector functions in glucose-deprived T cells.

The Glycoloytic Metabolite Phosphoenolpyruvate Regulates Ca^{2+}-NFAT Signaling in TH1 CD4+ T Cells by Inhibiting SERCA Activity

To determine which steps of glycolysis regulate cytoplasmic Ca^{2+} accumulation and T cell effector functions, TH1 cells were treated with 2-DG, iodoacetate (IAA) and oxalate (OXA), to inhibit hexokinase (HK), glyceraldehyde phosphate dehydrogenase (GAPDH), and pyruvate kinase (PK), respectively, at doses that showed comparable inhibition of lactate production (Figure 5A and data not shown). The glycolytic metabolites were examined by high-resolution liquid-chromatography Q-exactive mass spectrometry (LC-QE-MS) in the CD4+ T cells stimulated in the absence or presence of the inhibitors and as expected, the levels of 3- and 2-phosphoglycerate (3-PG/2-PG), and phosphoenolpyruvate (PEP) were suppressed by 2-DG and IAA, but promoted by OXA (Figures 5B and S5A). Interestingly,

2-DG and IAA, but not OXA, suppressed TH1 cell Ca^{2+} flux after ionomycin stimulation (Figure 5C) and CD40L and IFNγ production after TCR stimulation (Figures 5D and 5E). Likewise 2-DG and IAA, but not OXA, augmented TGFβ production (Figure 5F). These results suggested that a metabolite produced downstream of GAPDH and upstream of PK fine-tunes Ca^{2+} signaling and TH1 effector functions.

We hypothesized that such a metabolite may be PEP because of the above inhibitor studies and because TCR activation increases expression of the less-active M2 isoform of pyruvate kinase (PKM2) (Wang et al., 2011a), which allows the accumulation of several metabolic intermediates, including PEP, in proliferating cells (Vander Heiden et al., 2010). To more rigorously confirm the role of PEP in regulating the Ca^{2+}-NFAT pathway, we knocked down enolase 1 (Eno-1), the glycolytic enzyme that converts 2-PG into PEP (Figure S5B), and analyzed NFAT1 nuclear translocation and expression of IFNγ and CD40L in activated CD4+ T cells. This showed that NFAT1 nuclear translocation and the production of IFNγ and CD40L (Figures 5G and 5H) were greatly impaired by Eno-1 knock down. Additionally, treating TH1 CD4+ T cells with PKM2 activator DASS, which will decrease intracellular PEP levels (data not shown) (Anastasiou et al., 2012), similarly suppressed the production of IFNγ and CD40L (Figure S5C). Finally, supplementation of PEP (1 μg/ml), but not fosfomycin (a structurally related analog), to glucose-deprived CD4+ T cells restored Ca^{2+} flux in the presence of IAA (Figures 5I and S5D). Together these experiments narrowing in on the enzymes regulating PEP metabolism in cells, demonstrate that the accumulation of PEP is critical for sustaining Ca^{2+}-NFAT signaling.

To directly test if PEP can inhibit SERCA-mediated calcium uptake, we repeated the ER Ca^{2+} uptake assay by isolating ER vesicles from Jurkat T cells cultured in the presence or absence of glucose. This showed that glucose deprivation promoted ER Ca^{2+} uptake ability; however, PEP supplementation to the ER vesicle fraction significantly suppressed ER Ca^{2+} uptake indicating that PEP can inhibit SERCA activity (Figure 5J). Given that oxidation of SERCA on cysteine residues (e.g., Cys674 and Cys675) reduces SERCA activity (Sharov et al., 2006), we then examined whether glucose deprivation in T cells affects the redox state of SERCA using fluorescent thiol probes that measure the abundance of reduced cysteine residues on proteins. Jurkat T cells were cultured in glucose-replete or -deplete conditions, and ER vesicles were isolated and labeled with fluorescent probes that covalently bind to free thiols. SERCA was then immunoprecipitated from the ER vesicles and the amount of sample fluorescence measured indicated the abundance of reduced cysteines in SERCA. ER vesicles from glucose-deprived cells treated with H2O2 or β-mercaptoethanol (β-ME) served as positive controls for maximal cysteine oxidation and reduction, respectively. These experiments showed that compared to cells cultured in glucose-replete medium, glucose-deprivation increased the abundance of free thiols on SERCA, indicative of a more reduced state (Figure S5E). The addition of PEP, but not fosphomycin, to the ER vesicles decreased thiol abundance on SERCA similar to the amounts observed with H2O2 (Figure S5E). This result suggests that PEP likely impairs SERCA activity by promoting cysteine oxidation. To further explore this possibility, we found that treating glucose-deprived CD4+ T cells with H2O2, which suppresses SERCA activity via cysteine oxidation (Qin et al., 2013), could restore their ability to flux Ca^{2+} (Figure S5F). Collectively, these results identify a previously uncharacterized role for the metabolite PEP in controlling Ca^{2+} signaling through

inhibition, and likely the oxidation, of SERCA in T cells. These findings elucidate a nutrient-sensing mechanism by which T cells integrate their functional states with their metabolic states.

Metabolic Reprogramming of TILs Boosts Tumoricidal Activities in the Glucose-Deprived Tumor Microenvironment

The above findings support a model whereby the hyper-anabolic metabolic states of tumor cells reduce the availability of nutrients, such as glucose, and prevent TILs from sustaining Ca^{2+}-NFAT signaling and effector functions, in part, from PEP insufficiency. If so, it may be possible to metabolically reprogram anti-tumor T cells to increase their fitness and function in the tumor microenvironment. Because the data indicated that PEP was a critical metabolite controlling T cells function, we speculated that overexpression of phosphoenolpyruvate carboxykinase 1 (PCK1), which converts oxaloacetate (OAA) into PEP, could bolster the tumoricidal activity of TILs (Figure 6A). To examine this hypothesis, PCK1 (PCK1-OE) was overexpressed in Trp-1 CD4+ T cells specific for the melanoma antigen gp75/tyrosinase-related protein 1 (TRP-1), and this demonstrated that PCK1-OE specifically boosted PEP levels in T cells cultured in glucose-poor conditions (Figure 6B, compare blue and green bars), but had little effect on the amount of PEP above and beyond that normally found in T cells cultured in glucose-rich conditions. In contrast to control cells, PCK1-overexpression also reversed the effects of glucose-deprivation on Ca^{2+} flux and NFAT1 nuclear localization in CD4+ T cells (Figures 6C and 6D). It is important to note that the effects of glucose deprivation and PCK1-OE on CD8 T cell Ca^{2+} flux and effector functions were very similar to those observed in CD4 T cells. For example, blocking PEP accumulation via glycolytic inhibitors or PKM2 activators also diminished CD8+ T cell IFNγ production (Figures S6A and S6B). Additionally, PCK1-overexpression restored Ca^{2+} flux in glucose-deprived CD8+ T cells (Figure S6C). Thus, PCK1-OE lessened the dependence of both CD4 and CD8 T cells on glucose for Ca^{2+}-NFAT1 signaling in glucose-poor conditions.

Next, we examined whether PCK1-OE could enhance the anti-tumor responses of tumor-infiltrating Trp-1 CD4+ T cells. To this end, PCK1-OE or control Trp-1 CD4+ T cells were adoptively transferred into mice that contained engrafted B16 melanomas. Strikingly, PCK-OE increased Trp-1 CD4+ T cell production of IFNγ and CD40L over that of control cells in the tumors, but not in the spleen or draining lymph nodes where glucose is more abundant (Figure 6E). Additionally, relatively higher amounts of costimulatory ligand (CD86) and MHC class I and II expression were observed on TAMs in mice that received PCK1-OE Trp-1 CD4+ T cells compared to those that received control cells (Figure 6F), suggesting that restored effector functions by PCK1-OE Trp-1 CD4+ T cells promoted the maturation of TAMs. Most importantly, transfer of PCK1-OE Trp-1 CD4+ T cells suppressed melanoma growth (Figure 6G) and prolonged the survival of B16 melanoma-bearing mice (Figure 6H) compared to the control T cells. Of note, a similar suppression in tumor growth was observed in separate experiments when PCK1 was overexpressed in Pmel CD8+ T cells, specific for the melanoma antigen gp100 (Figures S6D and S6E). Taken together, our results provide strong evidence that metabolic reprogramming of both CD4 and CD8 T cells

is a promising strategy to boost effector functions of tumor-specific T cells in nutrient stressed conditions.

DISCUSSION

It is well appreciated that deregulated metabolism drives tumor cell growth, but it is underappreciated how this affects the metabolic or functional states of cells that infiltrate tumors (Pearce et al., 2013). Do cancer cells play a “metabolic tug-ofwar” with immune cells in tumors? Our work suggests they may because tumors with elevated rates of glycolytic activity were better able to elude T cell immunosurveillance. Further, TILs displayed signs of glucose deprivation, including impaired production of IFNγ and CD40L, but increased expression of TGFβ and genes associated with T cell anergy. This led to the discovery that glycolysis controls T cell Ca^{2+}-NFAT signaling and effector functions via the glycolytic metabolite PEP. Importantly, manipulation of this pathway by metabolically reprogramming TILs to increase PEP production yielded stronger anti-tumor responses. This work reveals that a glucose-poor tumor microenvironment can impose immunosuppressive properties on TILs and provides critical proof-of-concept evidence that metabolic reprogramming of tumor-specific T cells can be an adjunct form of immunotherapy.

In addition to other well-known immunosuppressive factors, our work indicates that glucose deprivation is another critical environmental restriction in solid tumors that restrains the tumoricidal functions of infiltrating tumor-specific CD4+ T cells. Support for this model also stems from studies showing that tumor-specific T cells regain effector function after being cultured in vitro for a short period of time (6–24 hr) in nutrient replete conditions (Wang et al., 2011b). Targeted inhibition of oncogenes, such as BrafV600E and KrasG12D, can stimulate T cell infiltration and production of IFNγ in tumors, and it is possible that these effects stem from their suppression of tumor cell aerobic glycolysis (Ho et al., 2014; Ying et al., 2012). However, further in vivo analyses are required to determine if tumor cells restrict glucose to infiltrating T cells through their own glycolytic activities and if this contributes to an immunosuppressive tumor microenvironment. Given that PD-1 signaling suppresses AktmTOR pathway and aerobic glycolysis (Parry et al., 2005; Staron et al., 2014), the therapeutic effects of anti-PD-1 immunotherapy will most certainly rely on TILs re-engaging aerobic glycolysis to regain proliferation and function. Indeed, rapamycin treatment abrogated the therapeutic effects of anti-PDL1 blockade on exhausted CD8 T cells during chronic viral infection (Staron et al., 2014). That both tumor cells and activated T cells share similar requirements for anabolic metabolism raises important considerations for designing drug treatments that combine metabolically targeted therapies with immunotherapy. For example, drugs that suppress tumor cell glycolysis may have poor efficacy long-term because of their unintended effects on TIL function. Therefore, as new treatments are tested, the effects of anti-cancer drugs on the metabolism and function of tumor infiltrating immune cells should be considered and examined.

It is clear that certain metabolic pathways serve as “metabolic checkpoints” to control T cell activation and function, but mechanistically how this occurs is not well understood. Our study uncovers a mechanism through which the glycolytic intermediate PEP regulates the amplitude of Ca^{2+} flux and NFAT activation to fine-tune T cell effector function. Although

PEP could inhibit SERCA activity and increase its oxidative state, the precise molecular mechanism(s) by which this occurs remains unknown. Possibly PEP directly conjugates to or oxidizes cysteine residues on SERCA or alternatively PEP could serve as a high-energy phosphate donor to phosphorylate SERCA or other proteins that inhibit its activity (Vander Heiden et al., 2010). Future biochemical studies are needed to precisely characterize which residues in SERCA, if any, are modified by PEP.

Metabolic flexibility allows activated T cells to adapt to changes in glucose availability by utilizing alternative substrates for energy production (Blagih et al., 2015; Frauwirth et al., 2002). Possibly, TILs become dependent on other carbon sources, such as lactic acid and free fatty acids (FFAs) abundant in the tumor microenvironment, and this not only changes the metabolic activities of TILs, but also their effector functions. Indeed, it is interesting to consider which carbon sources are used by the PCK-1 overexpressing T cells to manufacture PEP when glucose-deprived; our preliminary studies in vitro suggest that both lactic acid and FFAs may be involved (data not shown). Future in-depth metabolite profiling of TILs will help to characterize the nutrients they consume and the metabolic pathways they exercise in vivo, through which, one may develop more robust methods to harness anti-tumor T cell responses via metabolic manipulation.

Overall, our findings describe a metabolic checkpoint for T cell activity in tumors in which a glycolytic metabolite, PEP, serves as an intracellular sensor for glucose availability in the environment to regulate T cell activation and production of effector molecules. Together with another recent discovery identifying a secondary role for GAPDH in inhibiting IFNγ mRNA translation in T cells (Chang et al., 2013), these finding demonstrate that both metabolites and metabolic enzymes have adopted additional roles as metabolic checkpoint regulators to control specialized functions in T cells. From a therapeutic standpoint, better delineation of the metabolic pathways or enzymes differentially utilized by cancer cells and cancer-specific T cells could reveal vulnerable drug-targets in cancer cells. Additionally, rewiring the metabolic activity of TILs, as demonstrated herein and elsewhere (Doedens et al., 2013), could pose a new strategy for enhancing the potency and durability of ACT.

EXPERIMENTAL PROCEDURES

Mice, Tumor Engraftment, and Tumor Induction

The inducible mouse model of melanoma was previously described (Dankort et al., 2009) and Trp-1 TCR transgenic mice were purchased from Jackson Laboratory (Bar Harbor, ME). For melanoma cell engraftment, 2×105 B16 or Braf/Pten melanoma cells were suspended in 50 μl of PBS and then injected subcutaneously into wild-type C57BL/6 mice (Jackson Laboratory). All mouse experiments were performed according to the approved procedures of the Yale Institutional Animal Care and Use Committee.

ER Vesicle Isolation and Calcium Uptake Assay

Jurkat cells were cultured in glucose-free RPMI with 10% dialyzed FBS in the indicated conditions for 30 min. ER microsomal fractions were then isolated as previously described (Ho et al., 2011). ER vesicles were then analyzed by a calcium uptake assay with 45CaCl2

as the tracer of calcium uptake, as previously described (Borge and Wolf, 2003). For analysis of the effect of PEP on ER calcium uptake, the calcium uptake assay was performed in the presence of 6 μM PEP.

Fluorescence Labeling of SERCA Thiol Groups

ER microsomal fractions were then isolated from Jurkat cells cultured in glucose-free RPMI with 10% dialyzed FBS in 10 mM glucose or 0.1 mM glucose for 30 min. Two hundred micrograms of ER microsomal fraction was re-suspended in 20 mM sodium phosphate (pH7.4) buffer and then incubated with control vehicle, 1 μg/ml PEP, 1 μg/ml fosphomycin, 5 mM H2O2 or 1 mM β-mercaptoethanol for 10 min at 37°C. 200 mM Thiol-fluorescent probe IV (EMD Millipore, Billerica, MA) in the presence of 1% SDS for 30 min at 37°C. Then the reaction mixture was subjected for immunoprecipitation of SERCA or control IgG. The fluorescence intensity of the immunoprecipiates was then determined.

Statistical Analysis

Results were presented as mean ± SD or mean ± SEM and statistical significance was examined by an unpaired Student's t test. p value < 0.05 was considered as statistically significant.

Supplementary Material

Refer to Web version on PubMed Central for supplementary material.

ACKNOWLEDGMENTS

This study was supported in part by the Yale Cancer Center, Yale SPORE in Skin Cancer (5 P50 CA121974, R. Halaban, PI), Wade F.B. Thompson/Cancer Research Institute-CLIP grant, Howard Hughes Medical Institute, Melanoma Research Alliance (S.M.K), Melanoma Research Foundation (M.W.B), National Cancer Center (P-C.H.), CCFA award (284879, A.N.M.), Alliance for Lupus Research (J.C.R.) and NIH grants R37AI066232 and R01AI074699 to S.M.K., R01HL108006 to J.C.R., R00CA168997 and R01AI110613 to J.W.L.

REFERENCES

Anastasiou D, Yu Y, Israelsen WJ, Jiang JK, Boxer MB, Hong BS, Tempel W, Dimov S, Shen M, Jha A, et al. Pyruvate kinase M2 activators promote tetramer formation and suppress tumorigenesis. Nat. Chem. Biol. 2012; 8:839–847. [PubMed: 22922757]

Baitsch L, Fuertes-Marraco SA, Legat A, Meyer C, Speiser DE. The three main stumbling blocks for anticancer T cells. Trends Immunol. 2012; 33:364–372. [PubMed: 22445288]

Blagih J, Coulombe F, Vincent EE, Dupuy F, Galicia-Vázquez G, Yurchenko E, Raissi TC, van der Windt GJ, Viollet B, Pearce EL, et al. The energy sensor AMPK regulates T cell metabolic adaptation and effector responses in vivo. Immunity. 2015; 42:41–54. [PubMed: 25607458]

Borge PD Jr. Wolf BA. Insulin receptor substrate 1 regulation of sarco-endoplasmic reticulum calcium ATPase 3 in insulin-secreting beta-cells. J. Biol. Chem. 2003; 278:11359–11368. [PubMed: 12524443]

Braumüller H, Wieder T, Brenner E, Aßmann S, Hahn M, Alkhaled M, Schilbach K, Essmann F, Kneilling M, Griessinger C, et al. T-helper-1-cell cytokines drive cancer into senescence. Nature. 2013; 494:361–365. [PubMed: 23376950]

Callahan MK, Wolchok JD, Allison JP. Anti-CTLA-4 antibody therapy: immune monitoring during clinical development of a novel immuno-therapy. Semin. Oncol. 2010; 37:473–484. [PubMed: 21074063]

Cerami E, Gao J, Dogrusoz U, Gross BE, Sumer SO, Aksoy BA, Jacobsen A, Byrne CJ, Heuer ML, Larsson E, et al. The cBio cancer genomics portal: an open platform for exploring multidimensional cancer genomics data. Cancer Discov. 2012; 2:401–404. [PubMed: 22588877]

Cham CM, Driessens G, O'Keefe JP, Gajewski TF. Glucose deprivation inhibits multiple key gene expression events and effector functions in CD8+ T cells. Eur. J. Immunol. 2008; 38:2438–2450. [PubMed: 18792400]

Chang CH, Curtis JD, Maggi LB Jr. Faubert B, Villarino AV, O'Sullivan D, Huang SC, van der Windt GJ, Blagih J, Qiu J, et al. Post-transcriptional control of T cell effector function by aerobic glycolysis. Cell. 2013; 153:1239–1251. [PubMed: 23746840]

Dankort D, Curley DP, Cartlidge RA, Nelson B, Karnezis AN, Damsky WE Jr. You MJ, DePinho RA, McMahon M, Bosenberg M. Braf(V600E) cooperates with Pten loss to induce metastatic melanoma. Nat. Genet. 2009; 41:544–552. [PubMed: 19282848]

Doedens AL, Phan AT, Stradner MH, Fujimoto JK, Nguyen JV, Yang E, Johnson RS, Goldrath AW. Hypoxia-inducible factors enhance the effector responses of CD8(+) T cells to persistent antigen. Nat. Immunol. 2013; 14:1173–1182. [PubMed: 24076634]

Feske S, Skolnik EY, Prakriya M. Ion channels and transporters in lymphocyte function and immunity. Nat. Rev. Immunol. 2012; 12:532–547. [PubMed: 22699833]

Finlay DK, Rosenzweig E, Sinclair LV, Feijoo-Carnero C, Hukelmann JL, Rolf J, Panteleyev AA, Okkenhaug K, Cantrell DA. PDK1 regulation of mTOR and hypoxia-inducible factor 1 integrate metabolism and migration of CD8+ T cells. J. Exp. Med. 2012; 209:2441–2453. [PubMed: 23183047]

Frauwirth KA, Riley JL, Harris MH, Parry RV, Rathmell JC, Plas DR, Elstrom RL, June CH, Thompson CB. The CD28 signaling pathway regulates glucose metabolism. Immunity. 2002; 16:769–777. [PubMed: 12121659]

Gao J, Aksoy BA, Dogrusoz U, Dresdner G, Gross B, Sumer SO, Sun Y, Jacobsen A, Sinha R, Larsson E, et al. Integrative analysis of complex cancer genomics and clinical profiles using the cBioPortal. Sci. Signal. 2013; 6:pl1. [PubMed: 23550210]

Gubser PM, Bantug GR, Razik L, Fischer M, Dimeloe S, Hoenger G, Durovic B, Jauch A, Hess C. Rapid effector function of memory CD8+ T cells requires an immediate-early glycolytic switch. Nat. Immunol. 2013; 14:1064–1072. [PubMed: 23955661]

Gullino PM, Clark SH, Grantham FH. The Interstitial Fluid of Solid Tumors. Cancer Res. 1964; 24:780–794. [PubMed: 14190544]

Hanahan D, Weinberg RA. Hallmarks of cancer: the next generation. Cell. 2011; 144:646–674. [PubMed: 21376230]

Ho PC, Chuang YS, Hung CH, Wei LN. Cytoplasmic receptor-interacting protein 140 (RIP140) interacts with perilipin to regulate lipolysis. Cell. Signal. 2011; 23:1396–1403. [PubMed: 21504789]

Ho PC, Meeth KM, Tsui YC, Srivastava B, Bosenberg MW, Kaech SM. Immune-based antitumor effects of BRAF inhibitors rely on signaling by CD40L and IFNg. Cancer Res. 2014; 74:3205–3217. [PubMed: 24736544]

Macintyre AN, Gerriets VA, Nichols AG, Michalek RD, Rudolph MC, Deoliveira D, Anderson SM, Abel ED, Chen BJ, Hale LP, Rathmell JC. The glucose transporter Glut1 is selectively essential for CD4 T cell activation and effector function. Cell Metab. 2014; 20:61–72. [PubMed: 24930970]

MacIver NJ, Michalek RD, Rathmell JC. Metabolic regulation of T lymphocytes. Annu. Rev. Immunol. 2013; 31:259–283. [PubMed: 23298210]

Maude SL, Frey N, Shaw PA, Aplenc R, Barrett DM, Bunin NJ, Chew A, Gonzalez VE, Zheng Z, Lacey SF, et al. Chimeric antigen receptor T cells for sustained remissions in leukemia. N. Engl. J. Med. 2014; 371:1507–1517. [PubMed: 25317870]

Mellman I, Coukos G, Dranoff G. Cancer immunotherapy comes of age. Nature. 2011; 480:480–489. [PubMed: 22193102]

Michalek RD, Gerriets VA, Jacobs SR, Macintyre AN, MacIver NJ, Mason EF, Sullivan SA, Nichols AG, Rathmell JC. Cutting edge: distinct glycolytic and lipid oxidative metabolic programs are essential for effector and regulatory CD4+ T cell subsets. J. Immunol. 2011; 186:3299–3303. [PubMed: 21317389]

Moran AE, Holzapfel KL, Xing Y, Cunningham NR, Maltzman JS, Punt J, Hogquist KA. T cell receptor signal strength in Treg and iNKT cell development demonstrated by a novel fluorescent reporter mouse. J. Exp. Med. 2011; 208:1279–1289. [PubMed: 21606508]

Parry RV, Chemnitz JM, Frauwirth KA, Lanfranco AR, Braunstein I, Kobayashi SV, Linsley PS, Thompson CB, Riley JL. CTLA-4 and PD-1 receptors inhibit T-cell activation by distinct mechanisms. Mol. Cell. Biol. 2005; 25:9543–9553. [PubMed: 16227604]

Pearce EL, Poffenberger MC, Chang CH, Jones RG. Fueling immunity: insights into metabolism and lymphocyte function. Science. 2013; 342:1242454. [PubMed: 24115444]

Qin F, Siwik DA, Lancel S, Zhang J, Kuster GM, Luptak I, Wang L, Tong X, Kang YJ, Cohen RA, Colucci WS. Hydrogen peroxide-mediated SERCA cysteine 674 oxidation contributes to impaired cardiac myocyte relaxation in senescent mouse heart. J. Am. Heart Assoc. 2013; 2:e000184. [PubMed: 23963753]

Safford M, Collins S, Lutz MA, Allen A, Huang CT, Kowalski J, Black-ford A, Horton MR, Drake C, Schwartz RH, Powell JD. Egr-2 and Egr-3 are negative regulators of T cell activation. Nat. Immunol. 2005; 6:472–480. [PubMed: 15834410]

Schwartz RH. T cell anergy. Annu. Rev. Immunol. 2003; 21:305–334. [PubMed: 12471050]

Sharov VS, Dremina ES, Galeva NA, Williams TD, Schöneich C. Quantitative mapping of oxidation-sensitive cysteine residues in SERCA in vivo and in vitro by HPLC-electrospray-tandem MS: selective protein oxidation during biological aging. Biochem. J. 2006; 394:605–615. [PubMed: 16307534]

Shiao SL, Ganesan AP, Rugo HS, Coussens LM. Immune microenvironments in solid tumors: new targets for therapy. Genes Dev. 2011; 25:2559–2572. [PubMed: 22190457]

Smith-Garvin JE, Koretzky GA, Jordan MS. T cell activation. Annu. Rev. Immunol. 2009; 27:591–619. [PubMed: 19132916]

Srinivasan M, Frauwirth KA. Reciprocal NFAT1 and NFAT2 nuclear localization in CD8+ anergic T cells is regulated by suboptimal calcium signaling. J. Immunol. 2007; 179:3734–3741. [PubMed: 17785810]

Staron MM, Gray SM, Marshall HD, Parish IA, Chen JH, Perry CJ, Cui G, Li MO, Kaech SM. The transcription factor FoxO1 sustains expression of the inhibitory receptor PD-1 and survival of antiviral CD8(+) T cells during chronic infection. Immunity. 2014; 41:802–814. [PubMed: 25464856]

Vander Heiden MG, Locasale JW, Swanson KD, Sharfi H, Heffron GJ, Amador-Noguez D, Christofk HR, Wagner G, Rabinowitz JD, Asara JM, Cantley LC. Evidence for an alternative glycolytic pathway in rapidly proliferating cells. Science. 2010; 329:1492–1499. [PubMed: 20847263]

Wang R, Dillon CP, Shi LZ, Milasta S, Carter R, Finkelstein D, McCormick LL, Fitzgerald P, Chi H, Munger J, Green DR. The transcription factor Myc controls metabolic reprogramming upon T lymphocyte activation. Immunity. 2011a; 35:871–882. [PubMed: 22195744]

Wang SF, Fouquet S, Chapon M, Salmon H, Regnier F, Labroquère K, Badoual C, Damotte D, Validire P, Maubec E, et al. Early T cell signalling is reversibly altered in PD-1+ T lymphocytes infiltrating human tumors. PLoS ONE. 2011b; 6:e17621. [PubMed: 21408177]

Ward PS, Thompson CB. Metabolic reprogramming: a cancer hallmark even warburg did not anticipate. Cancer Cell. 2012; 21:297–308. [PubMed: 22439925]

Wherry EJ. T cell exhaustion. Nat. Immunol. 2011; 12:492–499. [PubMed: 21739672]

Wolchok JD, Kluger H, Callahan MK, Postow MA, Rizvi NA, Lesokhin AM, Segal NH, Ariyan CE, Gordon RA, Reed K, et al. Nivolumab plus ipilimumab in advanced melanoma. N. Engl. J. Med. 2013; 369:122–133. [PubMed: 23724867]

Yang M, Soga T, Pollard PJ. Oncometabolites: linking altered metabolism with cancer. J. Clin. Invest. 2013; 123:3652–3658. [PubMed: 23999438]

Ying H, Kimmelman AC, Lyssiotis CA, Hua S, Chu GC, Fletcher-Sananikone E, Locasale JW, Son J, Zhang H, Coloff JL, et al. Oncogenic Kras maintains pancreatic tumors through regulation of anabolic glucose metabolism. Cell. 2012; 149:656–670. [PubMed: 22541435]

Zheng Y, Delgoffe GM, Meyer CF, Chan W, Powell JD. Anergic T cells are metabolically anergic. J. Immunol. 2009; 183:6095–6101. [PubMed: 19841171]

Highlights

- Glucose deprivation suppresses anti-tumor T cell effector functions
- Glycolytic metabolite PEP sustains Ca^{2+} and NFAT signaling by blocking SERCA
- Ca^{2+} signaling is an integrator of glycolytic activity and TCR signaling
- T cell metabolic reprogramming enhances anti-tumor effector functions

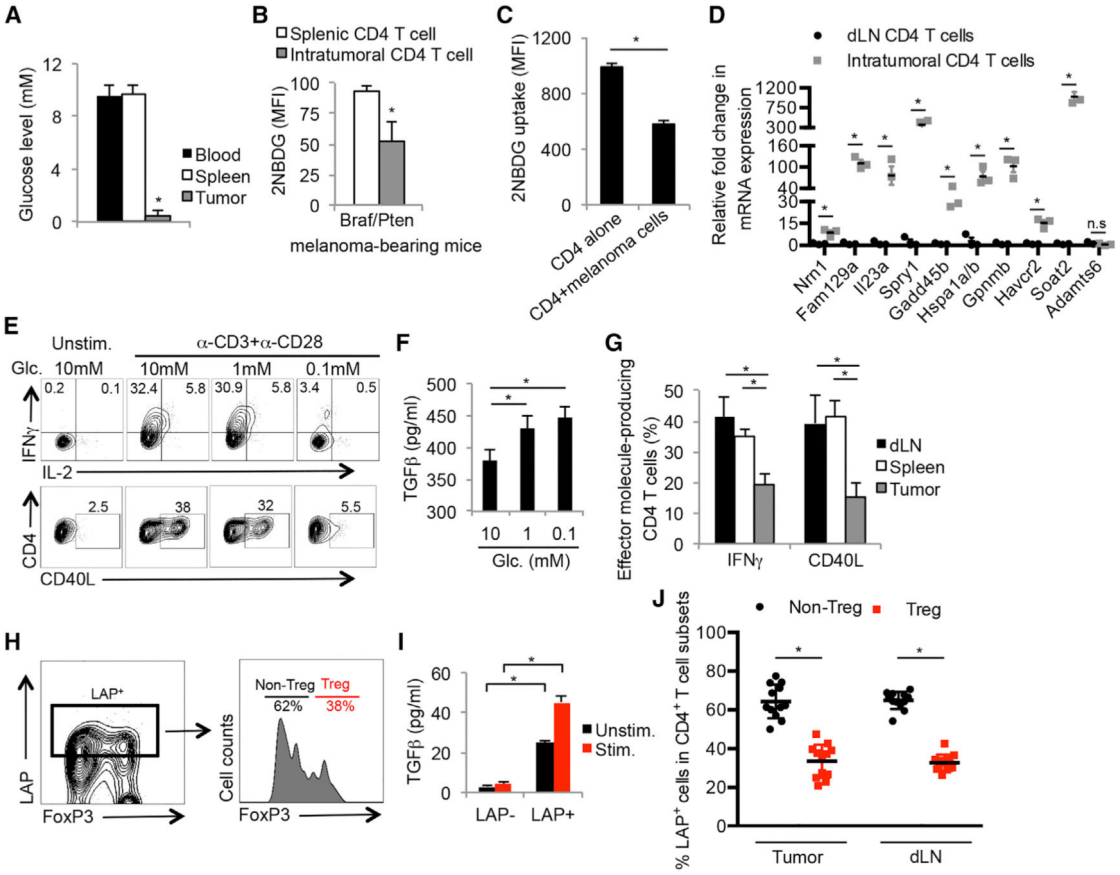

Figure 1. Tumor Microenvironment Deprives Glucose to Infiltrating CD4$^+$ T Cells

(A) Bar graphs show the glucose concentration in blood and interstitial fluid of tumors and spleens from Braf/Pten melanoma-bearing mice.

(B and C) Glucose uptake in splenic and intratumoral CD44$^+$/CD25^{lo} and CD44$^+$/CD25^{hi} CD4$^+$ T cells (B) or in T_H1 cells cultured with or without Braf/Pten melanoma cells (C) was determined using fluorescent 2-NBDG and measured by flow cytometry.

(D) The expression of glucose-deprived signature genes in CD4$^+$ T cells isolated from melanomas and draining lymph nodes (dLNs) was determined by qRT-PCR.

(E and F) T_H1 CD4$^+$ T cells derived from LCMV Armstrong-infected mice were stimulated by anti-CD3/anti-CD28 mAbs in vitro in the indicated glucose concentrations for 5 hr. The expression of IFNγ, IL-2, and CD40L was analyzed by flow cytometry (E), and production of TGFβ was determined by ELISA (F).

(G) The production of CD40L and IFNγ in CD4$^+$ T cells isolated from the dLN, spleen, or tumors in Braf/Pten mice was analyzed by flow cytometry.

(H) LAP surface expression was compared between activated FoxP3$^+$ (T_{reg}) and FoxP3$^-$ (non-T_{reg}) CD4$^+$ T cells within melanomas using flow cytometry.

(I) Validation of LAP staining as a surrogate for TGFβ secreting capability was performed by stimulating purified intratumoral LAP$^+$ and LAP$^-$ CD44$^+$ CD4 T$^+$ cells with or without anti-CD3/anti-CD28 mAbs for 16 hr and measuring the amount of TGFβ in culture supernatants by ELISA.

(J) The frequency of LAP^+ $FoxP3^+$ (T_{reg}) and $FoxP3^-$ (non-T_{reg}) $CD4^+$ T cells within melanomas or dLNs was assessed using flow cytometry.

Data shown are cumulative of two (A and B, D, H, I) (n = 3–6 mice/group/experiment) and three (G and J) independent experiments (n = 3–4 mice/group/experiment) or representative of three (C, E and F) independent experiments (n = 3–5/group). Data are expressed as mean ± SD and (C) is presented as mean ± SEM. *$p < 0.05$ by unpaired Student's t test.

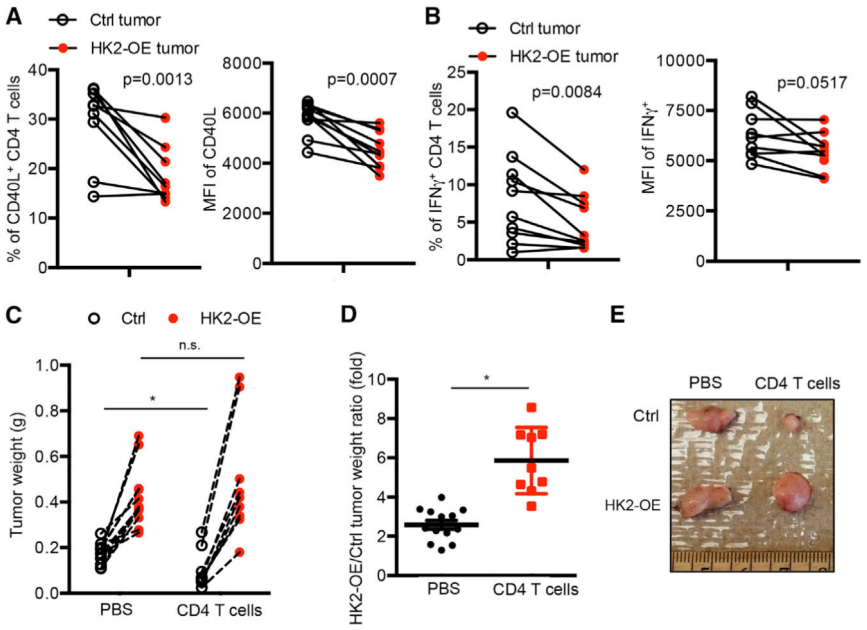

Figure 2. HK2 Overexpression in Melanoma Cells Suppresses CD4$^+$ T Cell-Mediated Anti-tumor Responses

(A and B) Control (Ctrl) or HK2-OE Braf/Pten tumors were engrafted into the right and left flanks of C57BL/6 mice. Fourteen days later, the CD4$^+$ TILs were isolated, stimulated in vitro by anti-CD3/anti-CD28 mAbs for 5 hr and analyzed for CD40L and IFNγ expression by flow cytometry. Left: percentage of CD40L$^+$ (A) or IFNγ$^+$ (B); right: mean fluorescence intensity (MFI) of the indicated proteins. (C–E) Ctrl or HK2-OE Braf/Pten tumors were engrafted into the right and left flanks of Rag1-KO mice mouse that were either injected with PBS or reconstituted with CD4$^+$ T cells and 14 days later the weight (C and D) and size (E) of tumors was assessed. (C and D) Graphs show tumor weights of the contralateral pairs of ctrl and HK2-OE melanomas collected from same mouse expressed as actual weights (C) or as a ratio (D).

Data shown are cumulative of three (A and B) independent experiments (n = 3–4 mice/group) or four (C and D) independent experiments (n = 2–4 mice/group). Data are expressed as mean ± SD and *p < 0.05 by unpaired Student's t test.

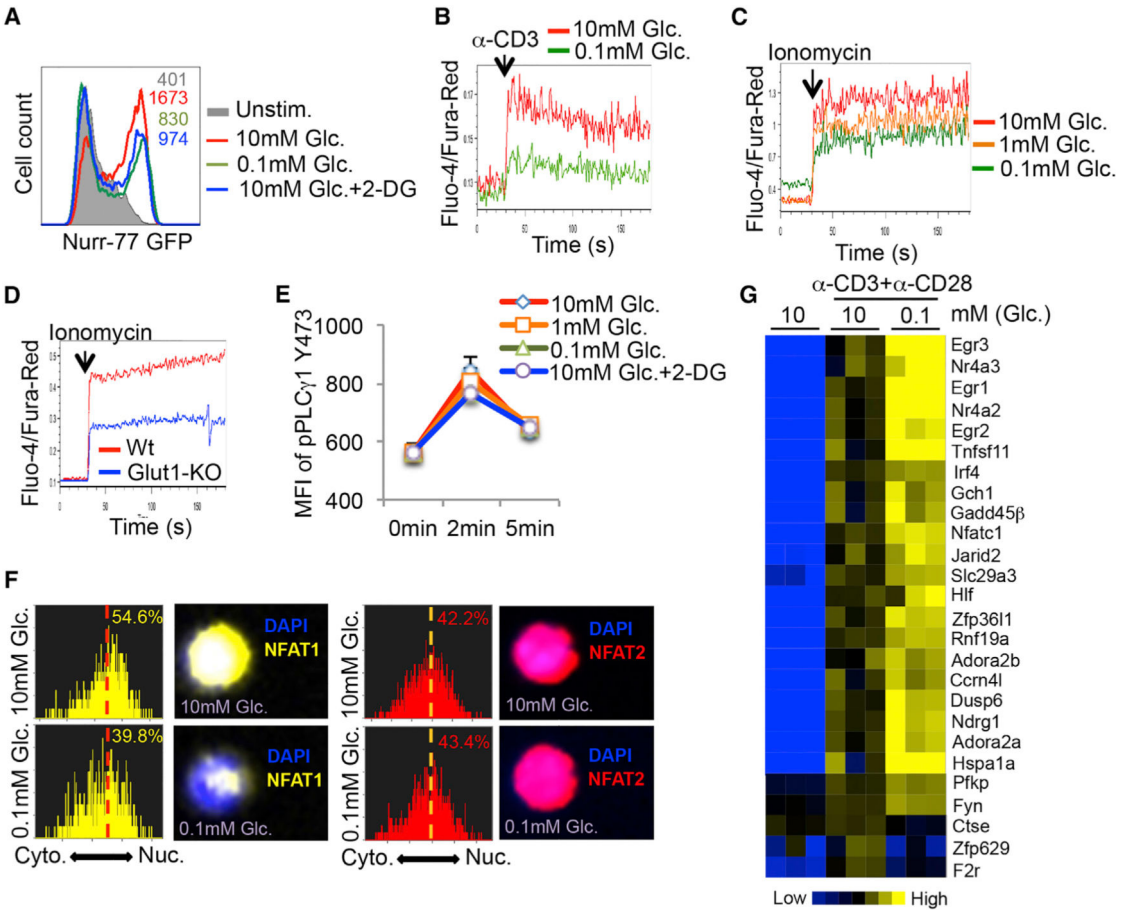

Figure 3. Glycolysis Modulates the Ca^{2+}-NFAT1 Signaling Pathway in CD4+ T Cells

(A) Naive CD4+ T cells from Nur-77-eGFP mice were left unstimulated or stimulated with anti-CD3/anti-CD28 mAbs for 5 hr in the indicated conditions and GFP fluorescence was measured by flow cytometry. Glc.: glucose; 2-DG: 2-deoxy-D-glucose.

(B and C) Intracellular Ca^{2+} levels were measured in Fluo-4- and Fura-Red-labeled TH1 CD4+ T cells cultured in 10 mM glucose or 0.1 mM glucose before and after activation with anti-CD3 crosslinking antibodies (B) or ionomycin (C). The ratio of Fluo-4 and Fura-Red fluorescence was measured using flow cytometry.

(D) Intracellular Ca^{2+} levels were measured as above in naive $CD4^+$ T cells isolated from wild-type (Wt) or GLUT-1-knockout (Glut1-KO) mice.

(E) T_H1 $CD4^+$ T cells were stimulated with anti-CD3/anti-CD28 in the indicated conditions and amounts of phospho-PLCγ1 were measured by flow cytometry.

(F) T_H1 cells were stimulated with ionomycin in medium containing 10 mM or 0.1 mM glucose for 10 min and the cytoplasmic versus nuclear distribution of NFAT1 and NFAT2 was determined by Amnis Imagestream. Representative histograms and images show the similarity profiles of NFAT1 (yellow, left) or NFAT2 (red, right) with DAPI staining to measure nuclear localization. The percentage of T cells with nuclear NFAT1 or NFAT2 is shown.

(G) Heat map shows normalized expression of select genes associated with T cell anergy (Safford et al., 2005) in T_H1 cells stimulated for 5 hr with anti-CD3/anti-CD28 mAbs in glucose-sufficient (10 mM) or glucose-deficient (0.1 mM) conditions.

Data shown are representative of two (D and E) and three (A–C, F) independent experiments or cumulative of three (G) independent experiments (n = 2 mice/group).

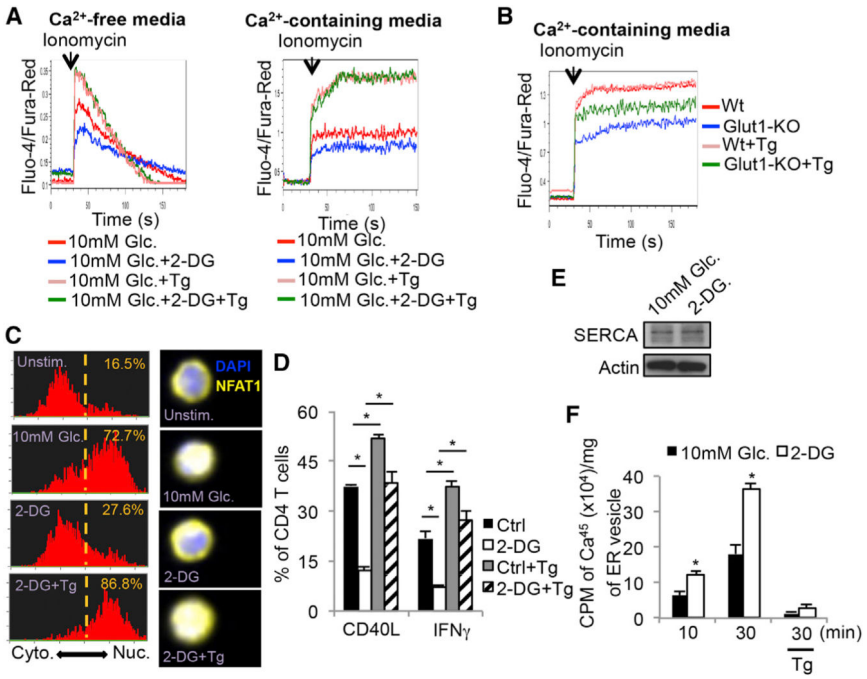

Figure 4. Glycolysis Sustains Cytoplasmic Ca^{2+} Accumulation via Modulation of SERCA-Mediated Calcium Reuptake

(A) Intracellular calcium levels were measured in Fluo-4- and Fura-Red-labeled CD4+ T cells cultured in Ca^{2+}-free (left) or Ca^{2+}-containing media (right) in 10 mM glucose or 2-DG with or without thapsigargin (Tg).

(B) Intracellular Ca^{2+} levels were measured as above in naive CD4+ T cells isolated from wild-type (Wt) or GLUT-1-knockout (Glut1-KO) mice and cultured in Ca^{2+}-containing media with or without Tg.

(C) Naive $CD4^+$ T cells were left unstimulated or stimulated with ionomycin in the presence of 10 mM glucose, 2-DG or 2-DG plus Tg for 10 min and the cytoplasmic versus nuclear distribution of NFAT1 was determined by Amnis Imagestream. Representative histograms (left) and images (right) show the similarity profiles of NFAT1/DAPI staining to measure NFAT1 nuclear localization. The frequency of T cells with nuclear NFAT1 is shown.

(D) Control or 2-DG treated T_H1 cells were stimulated with anti-CD3/anti-CD28 mAbs for 5 hr in the absence or presence of Tg. The expression of CD40L and IFNγ was analyzed by flow cytometry.

(E) Western blots showing the amount of SERCA protein in Jurkat T cells treated with or without 2-DG for 30 min.

(F) Ca^{2+}-uptake using radiolabeled 45CaCl2 was measured in ER microsomal fractions isolated from Jurkat T cells treated with or without 2-DG for 10 or 30 min.

Data shown are representative of two (E and F) and three (A and B, C–E) independent experiments (n = 3/group in D and F. Data are expressed as mean ± SD and *$p < 0.05$ by unpaired Student's t test.

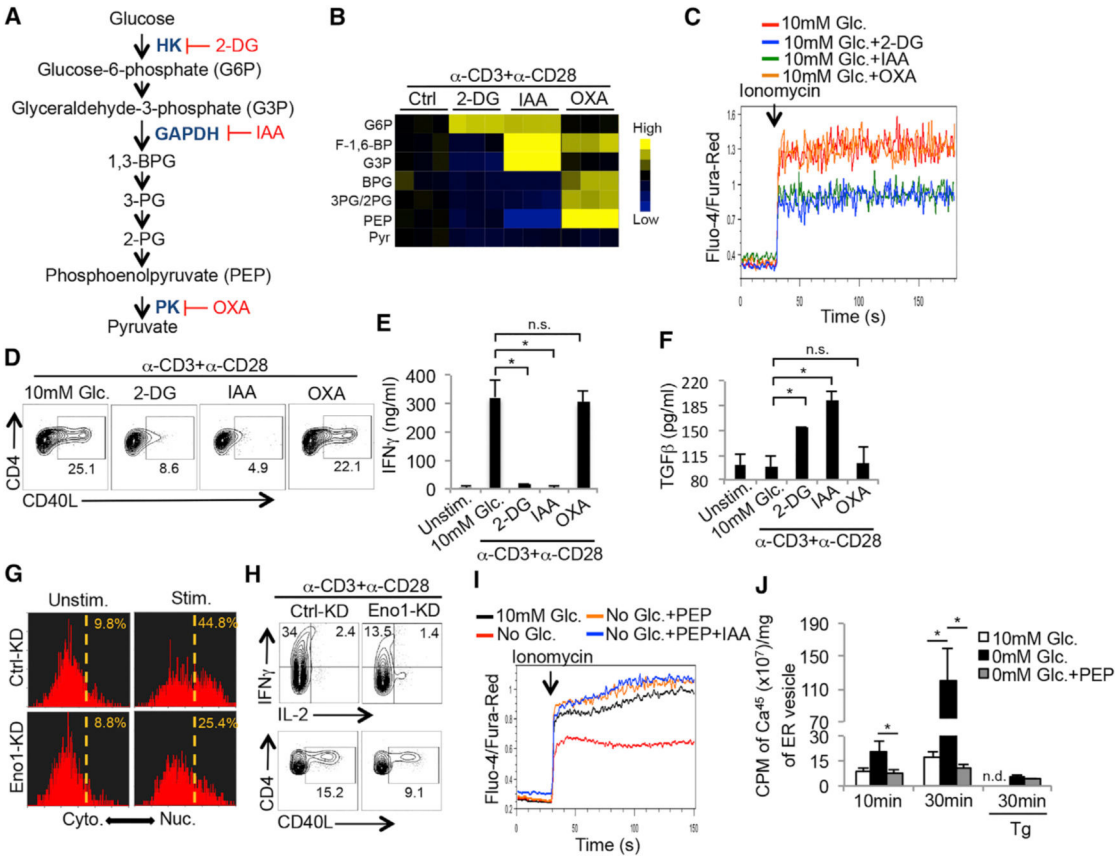

Figure 5. PEP Suppresses SERCA-Mediated ER Calcium Reuptake

(A) Illustration of the glycolysis pathway and the targets of the indicated glycolytic inhibitors. 2-DG: 2-deoxyglucose; IAA: iodoacetate; OXA: oxalate.

(B) Heat map shows the normalized concentrations of the indicated glycolytic metabolites in CD4+ T cells stimulated with anti-CD3/anti-CD28 mAbs for 1 hr in the absence or presence of the glycolytic inhibitors described in (A) as measured by LC-QE-MS.

(C) Intracellular Ca^{2+} levels were measured in Fluo-4- and Fura-Red-labeled T_H1 cells treated with indicated glycolytic inhibitors before and after activation with ionomycin.

(D–F) T_H1 cells were left alone or stimulated with anti-CD3/anti-CD28 mAbs for 5 hr in 10 mM glucose in the absence or presence of indicated glycolytic inhibitors and the expression of CD40L (D), IFNγ (E) and TGFβ (Φ) was measured by flow cytometry (D) or ELISA (E and F).

(G and H) $CD4^+$ T cells were transduced with empty vector control retroviruses (RV, Ctrl-KD) or those expressing enolase-1 shRNAi (eno1-KD). RV-infected T cells were left alone or stimulated with ionomycin for 10 min and the cytoplasmic versus nuclear distribution of NFAT1 was determined by Amnis Imagestream as described in Figure 3F (G), or alternatively were stimulated with anti-CD3/anti-CD28 mAbs in vitro in the presence of 10 mM glucose for 5 hr and the expression of IFNγ, IL-2 and CD40L was analyzed by flow cytometry (H).

(I) Intracellular Ca^{2+} levels in $CD4^+$ T cells that were partially permeabilized and recovered in the absence or presence of PEP were measured as in (C) in the absence or presence of glycolytic inhibitor IAA.

(J) Ca^{2+}-uptake assay as described in Figure 4F was performed on ER microsomal fractions isolated from Jurkat T cells cultured in the presence or absence of glucose or exogenous PEP. The addition of Tg served as a specificity control for SERCA-dependent activity.

Data shown are representative of two (H and J) and three (C and D, G and I) independent experiments or cumulative of three (B, E and F) independent experiments.

Data are expressed as mean ± SD and *$p < 0.05$ by unpaired Student's t test.

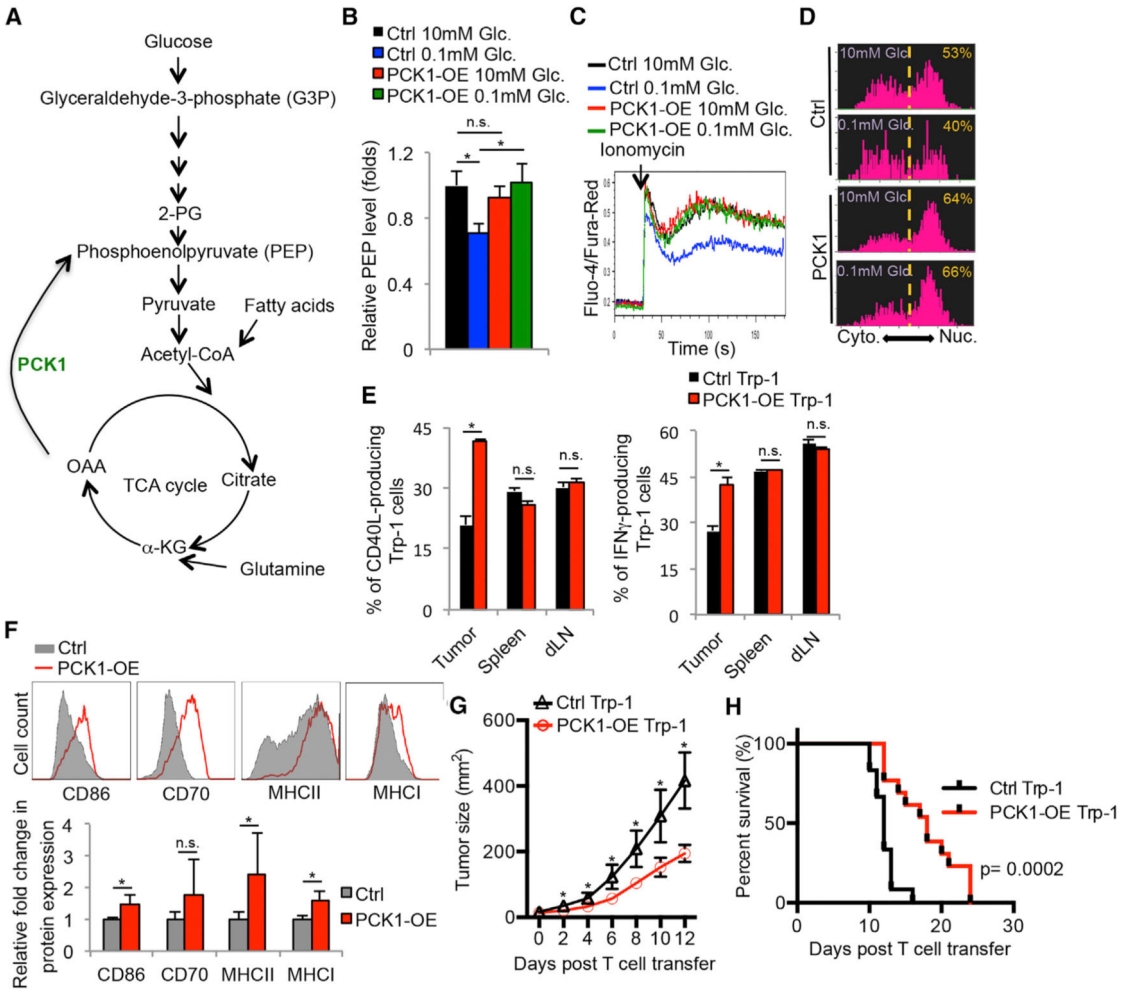

Figure 6. Overexpression of Phosphoenolpyruvate Carboxykinase 1 Boosts Ca2+-NFAT Signaling and Tumoricidal Activities of Tumor-Specific CD4+ T Cells

(A) Illustration of the metabolic function of PCK1 in converting OAA to PEP.

(B–D) CD4+ T cells were transduced with control (Ctrl) or PCK-1 overexpressing (PCK1-OE) RVs. (B) Intracellular PEP levels were measured after culturing the RV-transduced cells for 1 hr in the indicated conditions using a fluorescence-based assay. (C) Intracellular Ca^{2+} levels were measured in the transduced $CD4^+$ T cells cultured in 10 mM or 0.1 mM glucose before and after activation with ionomycin.

(D) The cytoplasmic versus nuclear distribution of NFAT1 was determined in the RV-transduced $CD4^+$ T cells stimulated with ionomycin in 10 mM glucose or 0.1 mM glucose for 10 min by Amnis Imagestream as described in Figure 5G.

(E–H) Melanoma-specific Trp-1^+ $CD4^+$ T cells transduced with Ctrl or PCK-1-OE RVs were adoptively transferred into B16 melanoma-bearing mice. (E and F) Three days later, the donor Trp-1^+ $CD4^+$ T cells (E) or TAMs (F) were isolated from the indicated tissues and analyzed for expression of the indicated proteins by flow cytometry. Rates of tumor growth (G) and animal survival (H) were determined over time.

Data shown are representative of two (D) and three (C) independent experiments or cumulative of two (F) (n = 2–3 mice/group/experiment), three (B, E) (n = 2–3 mice/group/

experiment), and four (G and H) independent experiments (n = 3–4 mice/group/experiment). Data are expressed as mean ± SD (B and F) or mean ± SEM (E) and *p < 0.05 by unpaired Student's t test.